expectation maximization corresponding to a pixel size of 4×4 mm, with section spacing of 2.66 mm.

PET data were evaluated semiquantitatively on the basis of the contrast ratio (CR) obtained as reported previously. Briefly, the regions of interest (ROIs) were chosen in the nodules or lymph nodes and cerebellum. The highest activities in the tumor or lymph node ROI (T or L) and in the cerebellum ROI (C) were measured. The CR was calculated by T/C in each nodule or L/C in each lymph node as an index of FDG-uptake. The primary tumors or lymph nodes with a CR ≥0.25 were diagnosed as having a viable tumor as reported previously.[7] The decrease in CR after neoadjuvant treatment was calculated using the following formula: CR after neoadjuvant treatment/CR before neoadjuvant treatment.

CT scanning and CT data analysis

Spiral CT was performed using a ProSeed SA (General Electric Health care, Milwaukee, Wisconsin, USA). The entire thorax was scanned in 1-cm-thick sections with maximal inspiration. World Health Organization (WHO) response criteria were used for efficacy analysis of the tumor.[8] The criterion of CT definition for suspected metastasis of the lymph node was a short-axis diameter of 1 cm or larger. The area of the tumor was calculated as the multiplication of the longest diameter and the shortest diameter. The decrease in tumor area on CT after neoadjuvant treatment was calculated using the following formula: tumor area after neoadjuvant treatment/tumor area before neoadjuvant treatment.

Pathologic response

Pathologic response was defined according to the article of The Japan Lung Cancer Society.[9] A major pathologic response was defined as a residual tumor less than one-third the size of the original tumor. A minor pathologic response was defined as residual tumor greater than or equal to one-third of the original tumor. The pathologic response was determined by comparing the ratios of FDG-uptake and tumor area on CT before and after neoadjuvant treatment in the 15 available patients.

Statistical analysis

True positive (TP), true negative (TN), false positive (FP) and false negative (FN) results of PET for residual tumor and lymph nodes were compared with the results of pathologic diagnosis. Sensitivity was calculated as TP/TP+FN, specificity as TN/TN+FP, positive predictive values (PPV) as TP/TP+FP, negative predictive values (NPV) as TN/TN+FN and accuracy as TP+TN/total. The differences between major pathologic response and minor pathologic response of the tumor by FDG-uptake and size on CT were examined by the Mann-Whitney *U* test. The data obtained by FDG-PET and CT were compared by the chi-squared test. The data were considered statistically significant at $p<0.05$. All values are expressed as the mean±SD.

Table 2. FDG-PET, CT, and residual viable tumor cells in the primary site

	Viable tumor cells	
	+	−
PET positive	16	2
PET negative	4	0
CT positive	20	2
CT negative	0	0

FDG-PET, ^{18}F-fluorodeoxyglucose positron emission tomography; CT, computed tomography.

Results

Detection of residual viable tumor at the primary site

While the effects of neoadjuvant treatment determined by CT were partial response in 12 and no change in 10 (Table 1), pathologic examination of the resected tumor showed that there were no viable cells in two patients. The results of the correlation between FDG-PET, CT and viable tumor cells are shown in Table 2. There were 16 patients with TP, four with FN and two with FP results by FDG-PET, 20 patients with TP and two patients with FP results by CT. There were no significant differences in the results of FDG-PET and CT.

Lymph node staging with PET and CT

A comparison of clinical (after neoadjuvant treatment) and pathologic lymph node status determined by FDG-PET and CT is shown in Table 3. FDG-PET and CT accurately predicted nodal status in 11 (50%) and 10 patients (45%), respectively. A comparison of clinical and pathologic node status in N1, N2 and N3 stations determined by FDG-PET and CT is shown in Table 4. Sensitivity, specificity, PPV, NPV and accuracy of FDG-PET and CT are summarized in Tables 5 and 6. PPV by FDG-PET (0.29) was significantly lower than that by CT (0.64) ($p=0.04$) in the N2 lymph node stations. However, there were no significant differences in the other results of FDG-PET and CT.

Table 3. Comparison of clinical and pathological nodal status by FDG-PET and CT

PET	Pathological nodal status			
	N0	N1	N2	N3
N0	5	2	2	0
N1	0	1	1	0
N2	2	3	4	1
N3	0	0	0	1

CT	Pathological nodal status			
	N0	N1	N2	N3
N0	5	2	2	0
N1	0	1	1	0
N2	2	3	4	2
N3	0	0	0	0

FDG-PET, ^{18}F-fluorodeoxyglucose positron emission tomography; CT, computed tomography.

Table 4. Comparisons between clinical and pathologic nodal status with FDG-PET and CT

		Lymph node metastasis	
		+	−
N1 station (n=24)	PET positive	4	5
	PET negative	1	14
	CT positive	2	1
	CT negative	3	18
N2 station (n=72)	PET positive	8	20
	PET negative	6	38
	CT positive	7	4
	CT negative	7	54
N3 station (n=7)	PET positive	2	0
	PET negative	2	3
	CT positive	0	0
	CT negative	4	3

FDG-PET, ^{18}F-fluorodeoxyglucose positron emission tomography; CT, computed tomography.

Table 5. The sensitivity, specificity, positive predictive value (PPV), negative predictive value (NPV) and accuracy for lymph node staging by FDG-PET after neoadjuvant treatment

Test	N1 lymph nodes	N2 lymph nodes	N3 lymph nodes	All lymph nodes
Sensitivity	0.80	0.57	0.50	0.61
Specificity	0.74	0.66	1.00	0.69
PPV	0.44	0.29	1.00	0.36
NPV	0.93	0.86	0.60	0.86
Accuracy	0.75	0.64	0.71	0.67

PPV, positive predictive value; NPV, negative predictive value; FDG-PET, ^{18}F-fluorodeoxyglucose positron emission tomography.

Table 6. The sensitivity, specificity, positive predictive value (PPV), negative predictive value (NPV) and accuracy for lymph node staging by CT after neoadjuvant treatment

Test	N1 lymph nodes	N2 lymph nodes	N3 lymph nodes	All lymph nodes
Sensitivity	0.40	0.50	0.00	0.39
Specificity	0.95	0.93	1.00	0.94
PPV	0.67	0.64	0.00	0.64
NPV	0.86	0.89	0.43	0.84
Accuracy	0.83	0.85	0.43	0.82

PPV, positive predictive value; NPV, negative predictive value; CT, computed tomography.

Pathologic response

In the 15 patients who underwent FDG-PET before and after neoadjuvant treatment, the ratios of FDG-uptake before and after neoadjuvant treatment in the major pathologic response patients (0.34±0.19) were significantly lower than those in the minor response patients (0.73±0.10)(p=0.003)(Fig. 1A). The ratios of tumor size on CT before and after neoadjuvant treatment in the major pathologic response patients (0.39±0.15) were also significantly lower than those in the minor pathologic response group (0.78±0.25)(p=0.009) (Fig. 1B). There was no significant difference in the ability of FDG-uptake or tumor size on CT to predict pathologic response.

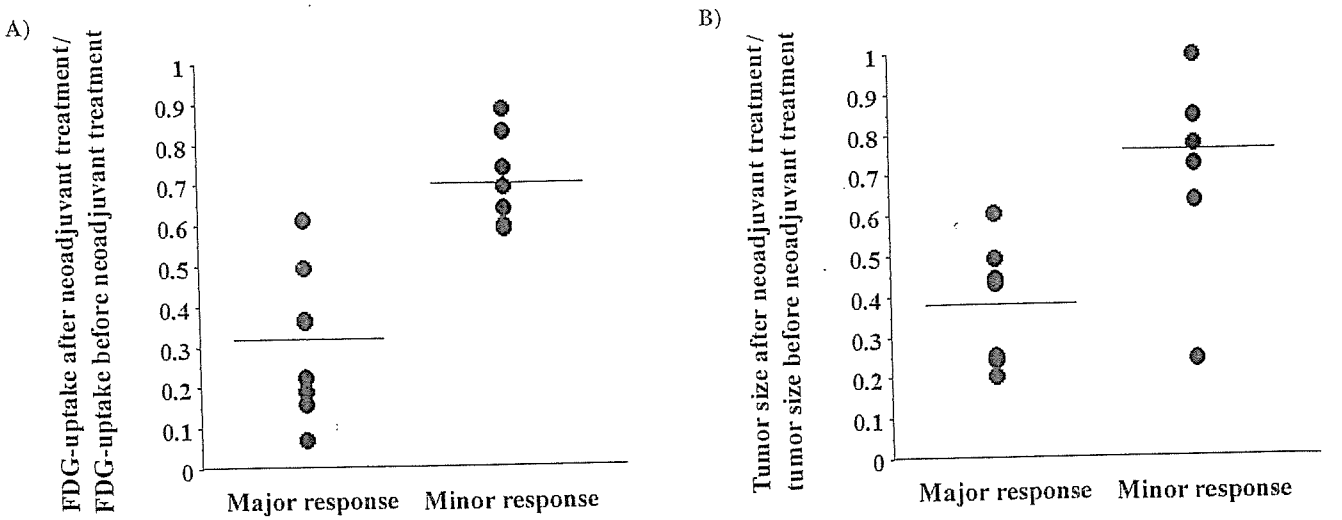

Fig. 1.

A: Distributions of the ratios of FDG-uptake in patients with a major and a minor pathologic response. The ratios of FDG-uptake in patients with a major pathologic response (0.34±0.19) were significantly lower than those in the group with minor pathologic response (0.73±0.10)(p=0.003).

B: Distributions of the ratios of the size in patients with a major and a minor pathologic response. The ratios of tumor size in patients with a major pathologic response (0.39±0.15) were also significantly lower than those in the group with minor pathologic response (0.78±0.25)(p=0.009).

Discussion

Surgical resection has limited success in curing locally advanced non-small cell lung cancer. Recently, combined modality treatment for locally advanced non-small cell lung cancer has been performed.[2] However, accurate staging of lung cancer is still difficult after neoadjuvant treatment.[10-12] FDG-PET, which does not use the criterion of size, might be more accurate for detecting the actual presence of tumor in the lymph nodes than CT. In mediastinal lymph node staging of lung cancer without neoadjuvant treatment, sensitivity and specificity are reported to be 0.71-0.91 and 0.67-0.94, respectively.[2-4,13] Several studies have shown good results for FDG-PET for the staging of lung cancer, even in patients who had received neoadjuvant treatment.[14-16] Akhurst et al. reported that FDG-PET could accurately detect residual viable primary tumor,[15] and Cerfolio et al. showed that FDG-PET had a higher PPV and NPV than CT for detecting residual tumor and paratracheal lymph nodes in patients who had received preoperative chemotherapy.[16] On the other hand, Port et al. reported that FDG-PET did not accurately predict nodal stage after neoadjuvant treatment.[17]

The current study showed that FDG-PET had a low PPV (0.29) when diagnosing mediastinal lymph nodes after neoadjuvant treatment. There were 20 FP lymph nodes (28%) among the 72 N2 lymph nodes. This poor result is thought to be due to inflammatory lesions with invasion of macrophages and lymphocytes in the lymph nodes caused by chemotherapy or radiation therapy. These lesions may be responsible for the increased uptake of FDG and the FP findings reported previously.[18]

Port et al. showed that FDG-PET did not reliably predict pathologic response to preoperative chemotherapy in non-small cell lung cancer.[17] However, the current study demonstrates that the FDG-uptake of the primary tumor before and after neoadjuvant treatment was a good predictor of pathologic response of the tumor. We defined a major pathologic response as 'residual tumor less than one-third the size of the primary tumor'. According to this definition, FDG-uptake could reflect the pathologic response of the primary tumor.

Lymph node downstaging of locally advanced non-small cell lung cancer by neoadjuvant treatment correlates with long-term survival.[19,20] FDG-PET did not offer any advantages over CT in the mediastinal lymph node and could not predict the lymph node downstaging of non-small cell lung cancer patients who received neoadjuvant treatment. Therefore, surgical intervention such as endoscopic biopsy or mediastinoscopy will be needed for accurate staging, since surgery after induction treatment is beneficial only in patients with pathologic downstaging.

References

1. Rosell R, Gomez-Codina J, Camps C, et al. A randomized trial comparing preoperative chemotherapy plus surgery with surgery alone in patients with non-small-cell lung cancer. *N Engl J Med* 1994; **330**: 153–8.
2. Dwamena BA, Sonnad SS, Angobaldo JO, Wahl RL. Metastases from non-small cell lung cancer: mediastinal staging in the 1990s—meta-analytic comparison of PET and CT. *Radiology* 1999; **213**: 530–6.
3. Gupta NC, Tamim WJ, Graeber GG, Bishop HA, Hobbs GR. Mediastinal lymph node sampling following positron emission tomography with fluorodeoxyglucose imaging in lung cancer staging. *Chest* 2001; **120**: 521–7.
4. Albes JM, Dohmen BM, Schott U, Schulen E, Wehrmann M, Ziemer G. Value of positron emission tomography for lung cancer staging. *Eur J Surg Oncol* 2002; **28**: 55–62.
5. Nomori H, Watanabe K, Ohtsuka T, Naruke T, Suemasu K, Uno K. The size of metastatic foci and lymph nodes yielding false-negative and false-positive lymph node staging with positron emission tomography in patients with lung cancer. *J Thorac Cardiovasc Surg* 2004; **127**: 1087–92.
6. Naruke T, Suemasu K, Ishikawa S. Lymph node mapping and curability at various levels of metastasis in resected lung cancer. *J Thorac Cardiovasc Surg* 1978; **76**: 832–9.
7. Nomori H, Watanabe K, Ohtsuka T, Naruke T, Suemasu K, Uno K. Visual and semiquantitative analyses for F-18 fluorodeoxyglucose PET scanning in pulmonary nodules 1 cm to 3 cm in size. *Ann Thorac Surg* 2005; **79**: 984–9.
8. WHO Handbook for Reporting Results of Cancer Treatment. Geneva: WHO, 1979.
9. The Japan Lung Cancer Society. General Rules for Clinical and Pathologic Recording of Lung Cancer, 6th ed. Tokyo: Kanehara, 2003. (in Jpse.)
10. Lee KS, Shim YM, Han J, et al. Primary tumors and mediastinal lymph nodes after neoadjuvant concurrent chemoradiotherapy of lung cancer: serial CT findings with pathologic correlation. *J Comput Assist Tomogr* 2000; **24**: 35–40.
11. Mateu-Navarro M, Rami-Porta R, Bastus-Piulats R, Cirera-Nogueras L, Gonzalez-Pont G. Remediastinoscopy after induction chemotherapy in non-small cell lung cancer. *Ann Thorac Surg* 2000; **70**: 391–5.
12. Van Schil P, van der Schoot J, Poniewierski J, et al. Remediastinoscopy after neoadjuvant therapy for non-small cell lung cancer. *Lung Cancer* 2002; **37**: 281–5.
13. Hellwig D, Ukena D, Paulsen F, Bamberg M, Kirsch CM, Onko-PET der Deutschen Gesellschaft fur Nuklearmedizin. [Meta-analysis of the efficacy of positron emission tomography with F-18-fluorodeoxyglucose in lung tumors. Basis for discussion of the German Consensus Conference on PET in Oncology 2000]. *Pneumologie* 2001; **55**: 367–77.
14. Vansteenkiste JF, Stroobants SG, De Leyn PR, Dupont PJ, Verbeken EK. Potential use of FDG-PET scan after induction chemotherapy in surgically staged IIIa-N2 non-small-cell lung cancer: a prospective pilot study. The Leuven Lung Cancer Group. *Ann Oncol* 1998; **9**: 1193–8.
15. Akhurst T, Downey RJ, Ginsberg MS, et al. An initial experience with FDG-PET in the imaging of residual disease after induction therapy for lung cancer. *Ann Thorac Surg* 2002; **73**: 259–66.
16. Cerfolio RJ, Ojha B, Mukherjee S, Pask AH, Bass CS, Katholi CR. Positron emission tomography scanning with 2-fluoro-2-deoxy-d-glucose as a predictor of response of neoadjuvant treatment for non-small cell carcinoma. *J Thorac Cardiovasc Surg* 2003; **125**: 938–44.
17. Port JL, Kent MS, Korst RJ, Keresztes R, Levin MA, Altorki NK. Positron emission tomography scanning poorly predicts response to preoperative chemotherapy in non-small cell lung cancer. *Ann Thorac Surg* 2004; **77**: 254–9.
18. Ohtsuka T, Nomori H, Watanabe K, et al. False-positive findings on ^{18}F-FDG-PET caused by non-neoplastic cellular elements after neoadjuvant chemoradiotherapy for non-small cell lung cancer. *Jpn J Clin Oncol* 2005; **35**: 271–3.
19. Betticher DC, Hsu Schmitz SF, Totsch M, et al. Mediastinal lymph node clearance after docetaxel-cisplatin neoadjuvant chemotherapy is prognostic of survival in patients with stage IIIA pN2 non-small-cell lung cancer: a multicenter phase II trial. *J Clin Oncol* 2003; **21**: 1752–9.
20. Trodella L, Granone P, Valente S, et al. Neoadjuvant concurrent radiochemotherapy in locally advanced (IIIA-IIIB) non-small-cell lung cancer: long-term results according to downstaging. *Ann Oncol* 2004; **15**: 389–98.

Jpn J Clin Oncol 2006;36(7)403–409
doi:10.1093/jjco/hyl043

Original Articles

[F-18]Fluorodeoxyglucose Positron Emission Tomography Can Predict Pathological Tumor Stage and Proliferative Activity Determined by Ki-67 in Clinical Stage IA Lung Adenocarcinomas

Ken-ichi Watanabe[1], Hiroaki Nomori[2], Takashi Ohtsuka[1], Tsuguo Naruke[1], Akinori Ebihara[1], Hideki Orikasa[3], Kazuto Yamazaki[3], Kimiichi Uno[4], Toshiaki Kobayashi[5] and Tomoyuki Goya[6]

[1]Department of Thoracic Surgery and Respiratory Group, Saiseikai Central Hospital, Tokyo, [2]Department of Thoracic Surgery, Graduate School of Medicine, Kumamoto University, Kumamoto, [3]Department of Pathology, Saiseikai Central Hospital, Tokyo, [4]Nishidai Clinic, Tokyo, [5]Development in Assistive Diagnostic Technology, National Cancer Center Hospital, Tokyo and [6]Department of Surgery, Kyorin University, Mitaka, Tokyo, Japan

Received December 18, 2005; accepted April 3, 2006; published online June 16, 2006

Objective: To predict a malignant grade of lung cancer by fluorodeoxyglucose positron emission tomography (FDG-PET) scanning, we investigated the correlation between FDG uptake and pathological tumor stage, proliferative activities determined by Ki-67 and cyclin D1, and an alteration of p53, in clinical stage (c-stage) IA lung adenocarcinomas.
Methods: FDG-PET was performed for 71 patients with c-stage IA lung adenocarcinomas. FDG uptake was measured by a contrast ratio (CR) between the tumor and contralateral lung. Ki-67, cyclin D1 and p53 staining scores were examined by immunohistochemistry.
Results: The lesions with ground-glass opacity were found in 26 patients, and solid lesions in 45 by computed tomography. The pathological tumor stages (p-stage) were stage IA in 59 and more advanced stages in 12. The latter had significantly higher CR value than the former ($P < 0.001$). Patients with CR $\geqslant$ 0.55 could be predicted to be at advanced tumor stages, with a sensitivity of 0.83 and a specificity of 0.82. The CR and staining scores of Ki-67 were significantly correlated with each other ($P < 0.0001$), and both the values were significantly higher in advanced tumor stages than in p-stage IA, and were also significantly higher in tumors with intratumoral lymphatic, vascular and pleural involvements than in those without such features ($P < 0.05$–0.0001).
Conclusions: In c-stage IA lung adenocarcinomas, the FDG uptake can predict p-stage and tumor proliferative activity determined by Ki-67. For c-stage IA lung adenocarcinomas showing CR $\geqslant$ 0.55, mediastinoscopy or neoadjuvant chemotherapy is indicated.

Key words: positron emission tomography – lung cancer – adenocarcinoma – tumor stage – proliferative activity – tumor suppressor gene

INTRODUCTION

It has been reported that tumor proliferative activity and alterations of tumor suppressor genes could be prognostic factors in non-small cell lung cancer (NSCLC). Some authors have demonstrated that proliferative activities determined by Ki-67 (1) and cyclin D1 (2–5), and an alteration of p53 were correlated with the prognosis of NSCLC patients (4,6,7). In recent years, F-18 fluorodeoxyglucose positron emission tomography (FDG-PET) has been frequently used for the diagnosis and staging of lung cancer (8–10). FDG uptake has been reported to be correlated not only with the prognosis in NSCLC patients (11,12) but also with the proliferative activity (13,14) and alteration of p53 (7) of the tumor. However, we previously reported that the FDG uptake in NSCLC tumors was dependent on histological types, that is, FDG-uptake of adenocarcinomas correlated with the pathological tumor stage and tumor invasiveness, but that of the other histological types did not (15,16). Therefore, we consider that the correlation between the FDG

For all reprints and all correspondence: Hiroaki Nomori, Department of Thoracic Surgery, Graduate School of Medicine, Kumamoto University, 1-1-1, Honjo, Kumamoto 860-8556, Japan; E-mail: hnomori@kaiju.medic.kumamoto-u.ac.jp

uptake and the proliferative activity or alteration of p53 should be examined in adenocarcinomas, but not in NSCLC including all histological types. Furthermore, FDG uptake is known to be higher in larger tumors (17,18). Therefore, in the present study, we measured the FDG uptake in clinical stage IA adenocarcinomas and investigated its relationships with the pathological tumor stage, intratumoral invasiveness, proliferative activity determined by Ki-67 and cyclin D1 and the alteration of p53.

PATIENTS AND METHODS

PATIENTS

Between December 2001 and February 2005, FDG-PET was performed for 386 patients with pulmonary nodules. Of these, 301 patients had malignant tumors and 178 of the 301 patients had lung adenocarcinoma. Of the 178 adenocarcinoma patients, 77 were diagnosed as clinical stage IA by PET and thin section computed tomography (TSCT: <2 mm in thickness). They were treated by segmentectomy or lobectomy and lymph node dissection. Of these, we excluded six adenocarcinomas < 1 cm, because the spatial resolution of the PET scanner is 0.7–0.8 cm, making it difficult to image the pulmonary nodules that are <1 cm (16). Therefore, we studied 71 patients with clinical stage IA adenocarcinoma with a size range of 1–3 cm.

FDG-PET SCANNING

Patients were instructed to fast for at least 4 h before intravenous (i.v.) administration of F-18 FDG. The dosage of F-18 FDG administered was 125 μCi/kg (4.6 MBq/kg) for non-diabetic patients and 150 μCi/kg (5.6 MBq/kg) for diabetic patients. PET imaging was performed ~60 min after administration of FDG with a POSICAM.HZL m-POWER (Positron Co., Houston, TX, USA). No attenuation-corrected emission scans were initially obtained in two-dimensional, high-sensitivity mode for 4 min per bed position, and taken from the vertical skull through the mid-thighs. Immediately thereafter, a two-bed-position attenuation-corrected examination was performed with 6 min for the emission sequence and 6 min for the transmission sequence at each bed position.

PET IMAGE PROCESSING AND DATA ANALYSIS

The images were usually reconstructed in a 256 × 256 matrix by using ordered subset expectation maximization corresponding to a pixel size of 4 × 4 mm, with section spacing of 2.66 mm. FDG uptake was evaluated by contrast ratio (CR) with contralateral lung, as previously reported (15,16,19). Briefly, the regions of interest (ROI) were placed in the nodules and contralateral normal lung. Highest standardized uptake ratios in the tumor ROI (T) and in the contralateral lung ROI (N) were measured. The CR value was calculated by using the formula $[(T - N)/(T + N)]$ in each nodule as an index of FDG uptake.

PATHOLOGICAL ANALYSIS

Hematoxylin and eosin and Elastica-van Gieson stainings were performed in all sections to investigate the intratumoral lymphatic and vascular invasions and pleural involvement. Pleural involvement was classified as p0, p1, p2 and p3; that is, a p0 tumor did not extend beyond the pleural elastic layer; a p1 tumor invaded the visceral pleural elastic layer, but did not reach the pleural surface; a p2 tumor included tumor exposure on the pleural surface; and a p3 tumor invaded the parietal pleura or the chest wall. The tumor stages were based on the TNM classification of the International Union Against Cancer (20): p2 tumors were classified as T2, p3 tumors were classified as T3 and tumors with intrapulmonary metastases within the same lobe were classified as T4.

PREDICTING ADVANCED TUMOR STAGES FROM FDG UPTAKE

Receiver operating characteristics (ROC) curve (21) was constructed according to the CR value, and the cut-off value was determined for predicting the pathological stages that were more advanced than stage IB.

IMMUNOHISTOCHEMICAL ANALYSIS

Immunostaining was performed by using the Dako envision system (Dako Cytomation, Glostrup, Denmark). The antibodies for Ki-67(monoclonal mouse antibody MIB-1, 1 : 100 dilution), cyclin D1 (monoclonal mouse antibody DCS-1, 1 : 50 dilution) and p53 (monoclonal mouse antibody, DO7, 1 : 400 dilution) were purchased from Dako Co. Sections of 4 μm were cut from the paraffin blocks. Immunostaining was performed with antigen-retrieval techniques.

EVALUATION OF IMMUNOHISTOCHEMICAL STAINING

Ki-67

According to the method of Martin et al. (1), the labeling index of Ki-67 was measured by determining the percentage of cells with positive nuclei in >1000 tumor cells in >4 fields.

Cyclin D1 and p53

The Allred score used to examine the staining scores of cyclin D1 as well as p53 was obtained by determining the percentage of positive tumor cells and staining intensity (22). Briefly, a percentage score was measured by determining the percentage of positive tumor cells in >1000 tumor cells in >4 fields (0, none; 1, <1/100; 2, 1/100–1/10; 3, 1/10–1/3; 4, 1/3–2/3; 5, >2/3). An intensity score was measured by the average of staining intensity (0, none; 1, weak; 2, intermediate; and 3, strong). The sum of the percentage score and the intensity score was used as the Allred score.

STATISTICAL ANALYSIS

The values of CR and staining scores of Ki-67, cyclin D1 and p53 were compared between the pathological stage IA and the

Table 1. Patients' characteristics

Gender	
Male	45
Female	26
Age (years)	62 ± 10 (33–83)*
Size (mm)	19 ± 7 (10–30)*
CT findings	
GGO	26
Solid	45
Pathological stage	
IA	59
≥IB	12
T2N0M0	3
T1N1M0	4
T2N1M0	1
T1N2M0	1
T4N0M0	2
T4N2M0	1

*Mean ± standard deviation (range), GGO: ground-glass opacity.

more advanced stages and between the two groups with or without intratumoral lymphatic, vascular invasion and pleural involvement, by the non-parametric Mann–Whitney's *U*-test. The correlations between the CR values and the staining scores of Ki-67, cyclin D1 and p53 were analyzed by using the non-parametric Spearman's rank test. All values in the text and tables are given as mean ± standard deviation.

RESULTS

Table 1 shows patients' characteristics. The lesion showing ground-glass opacity (GGO) image were found in 26 patients, and the solid lesions in 45 patients at visual TSCT findings. The pathological tumor stages were T1N0M0 in 59 patients and more advanced in 12 patients (i.e. T2N0M0 in 3, T1N1M0 in 4, T2N1M0 in 1, T1N2M0 in 1, T4N0M0 in 2 and T4N2M1 in 1).

Figure 1 shows the distribution of CR values in 59 patients with pathological stage IA and 12 patients with more advanced stages. The mean CR value of the 12 patients with advanced stages was 0.66 ± 0.12, which was significantly higher than 0.32 ± 0.18 of the 59 patients with pathological stage IA ($P < 0.001$).

Figure 2 depicts the ROC curve for predicting tumor stages more advanced than IB, showing the optimal CR cut-off value to be 0.55, of which sensitivity, specificity and accuracy were 0.83, 0.81 and 0.82, respectively. While 10 of the 12 patients (83%) with the advanced stage showed CR values ≥ 0.55, 48 of the 59 patients (81%) with pathological stage IA showed CR values < 0.55 (Table 2).

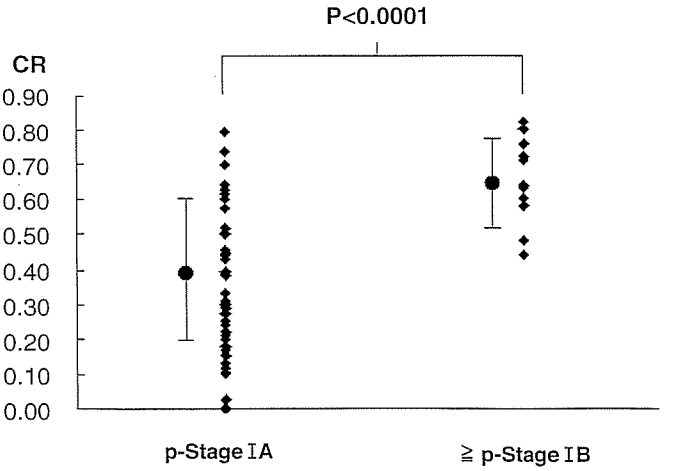

Figure 1. The distribution of CR values in the 59 patients with pathological stage IA and 12 patients with stages advanced more than IA. (CR = contrast ratio).

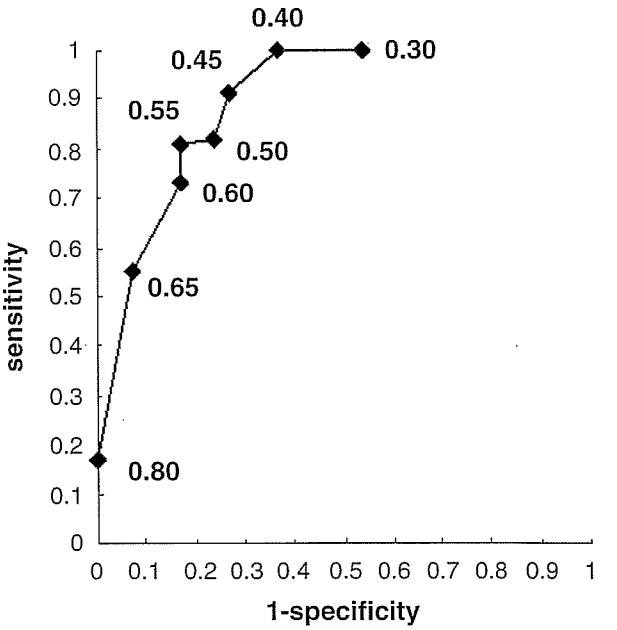

Figure 2. The ROC curve and CR values for predicting tumor stages more advanced than IA. (ROC = receiver operating characteristics; CR = contrast ratio).

Figures 3–5 show the distribution of staining scores of Ki-67, cyclin D1 and p53 in the 59 patients with pathological stage IA and 12 patients with more advanced stages. The mean score for Ki-67 in the 12 patients with advanced stages was 18.0 ± 11.0, which was significantly higher than 9.4 ± 12.0 for the 59 patients with pathological stage IA ($P = 0.012$). However, the mean scores for cyclin D1 in the advanced tumor stages and pathological stage IA were 3.9 ± 1.7 and 4.1 ± 1.8, respectively, of which difference was not significant. The mean scores for p53 in the advanced tumor stages and pathological stage IA were 3.3 ± 3.6 and 2.6 ± 2.6, respectively, of which difference was also not significant.

Table 2. Pathological tumor stage with the cut-off value of CR at 0.55

Pathological tumor stage	CR ≥ 0.55	CR < 0.55	Total
IA	11	48	59
≥IB	10	2	12
Total	21	50	71

≥IB: advanced stage more than IB.

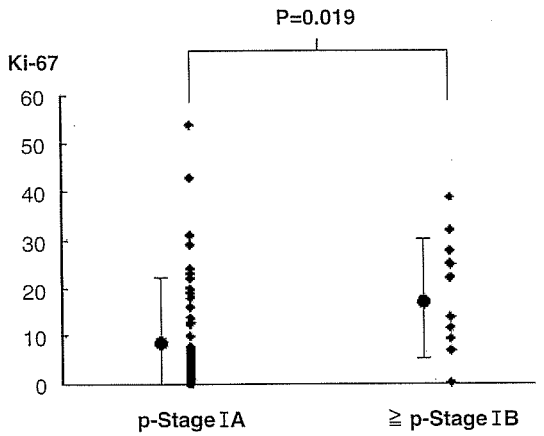

Figure 3. The distribution of Ki-67 staining scores in the 59 patients with pathological stage IA and 12 patients with stages advanced more than IA.

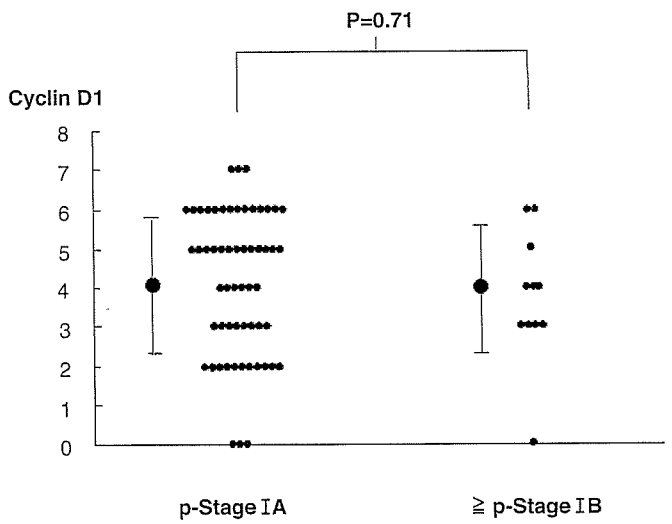

Figure 4. The distribution of cyclin D1 staining scores in the 59 patients with pathological stage IA and 12 patients with stages advanced more than IA.

Table 3 shows the mean values of CR, Ki-67, cyclin D1 and p53 staining scores in tumors with or without intratumoral lymphatic, vascular and pleural involvements. Tumors with intratumoral lymphatic, vascular and pleural involvements had significantly higher values of both CR and Ki-67 staining scores ($P < 0.05$–0.001). However, there were no significant differences of tumor invasiveness in the cyclin D1 and p53 staining scores.

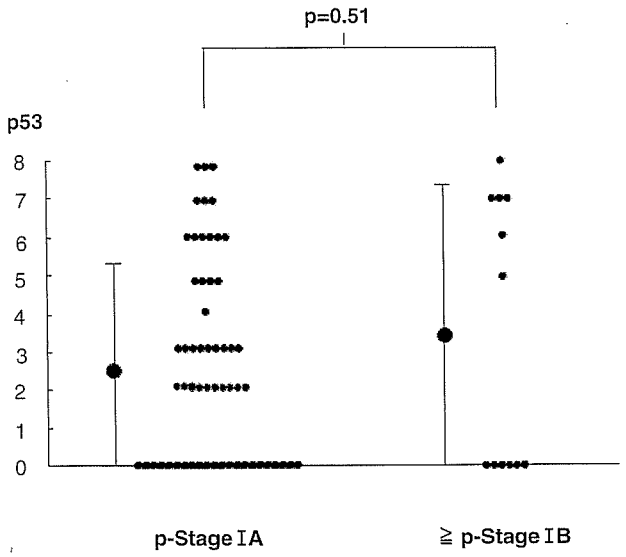

Figure 5. The distribution of p53 staining scores in the 59 patients with pathological stage IA and 12 patients with stages advanced more than IA.

Table 4 shows the mean values of CR and Ki-67 staining scores in tumors with stage IA and advanced stages in tumors with GGO and solid images. In 26 tumors with GGO image, 25 were stage IA and the other one was stage IB. The GGO tumors showed significantly lower CR and Ki-67 staining scores than the solid tumors ($P < 0.001$). The mean values of CR of the 25 GGO tumors with stage IA was 0.17 ± 0.14, while the CR of the one tumor with stage IB was 0.48. The mean values of Ki-67 staining scores of the 25 GGO tumors with stage IA was 4.7 ± 6.9, while the CR of the one tumor with stage IB was 0.16. In 45 tumors with solid image, 34 were stage IA and 11 were more advanced than stage IB. The mean values of CR of the 34 solid tumors with stage IA was 0.43 ± 0.20, which was significantly lower than 0.67 ± 0.11 of the 11 tumors with more advanced stages ($P < 0.001$). The mean values of Ki-67 staining scores of the 34 solid tumors with stage IA was 13 ± 13, which was lower than 21 ± 10 of the 11 solid tumors with more advanced stages ($P = 0.056$).

The CR value and Ki-67 staining scores were significantly correlated with each other ($r = 0.42$, $P < 0.0001$) (Fig. 6). However, both cyclin D1 and p53 scores did not show any correlation with the CR values ($r = 0.05$ and 0.07, respectively).

DISCUSSION

Although the standard uptake value (SUV) has been frequently used for evaluation of FDG-PET, it has been reported that several factors can affect the SUV, such as body size (23), blood glucose level (24), time after injection (25) and lesion size (17,18). In fact, the mean SUV of malignant pulmonary nodules has been reported to be various, ranging from 5.5 to 10.1 (26–29). We previously compared the results of SUV, CR with contralateral lung and CR with cerebellum for pulmonary nodules, and reported that the CR with contralateral lung or

Table 3. Correlation between intratumoral invasiveness and CR values and staining scores of Ki-67, cyclin D1 and p53

Invasiveness	Number of patients	CR	Ki-67	p53	Cyclin D1
ly (−)	38	0.29 ± 0.21	5.6 ± 8.1	2.2 ± 2.3	3.9 ± 1.8
(+)	33	0.48 ± 0.21*	17 ± 13*	3.4 ± 3.1	4.3 ± 1.8
v (−)	58	0.34 ± 0.23	9.9 ± 12	2.9 ± 2.7	4.1 ± 1.8
(+)	13	0.55 ± 0.20**	17 ± 12***	2.1 ± 3.0	3.8 ± 1.7
p 0	63	0.34 ± 0.20	9.7 ± 12	2.5 ± 2.6	4.1 ± 1.8
1–2	8	0.63 ± 0.13*	21 ± 8.3**	4.5 ± 3.6	3.8 ± 2.0

CR, contrast ratio; ly, lymphatic invasion; v, vascular invasion; p, pleural involvement.
*$P < 0.001$.
**$P < 0.01$.
***$P < 0.05$.

Table 4. The values of CR and Ki-67 of tumors with stage IA and advanced stages in tumors with solid and GGO images

Tumor findings and pathological stage	CR	Ki-67
GGO		
All cases ($n = 26$)	0.18 ± 0.14	4.5 ± 6.8
Stage IA ($n = 25$)	0.17 ± 0.14	4.7 ± 6.9
Stage IB ($n = 1$)	0.48	0.16
Solid		
All cases ($n = 45$)	0.48 ± 0.2*	15 ± 13*
Stage IA ($n = 34$)	0.43 ± 0.20	13 ± 13
⩾Stage IB ($n = 11$)	0.67 ± 0.11†	21 ± 10

GGO, ground-glass opacity; CR, contrast ratio.
*The differences of CR or Ki-67 staining scores between the GGO and solid lesions were $P < 0.001$.
†The difference of CR between the tumors with stage IA and ⩾stage IB was $P < 0.001$.

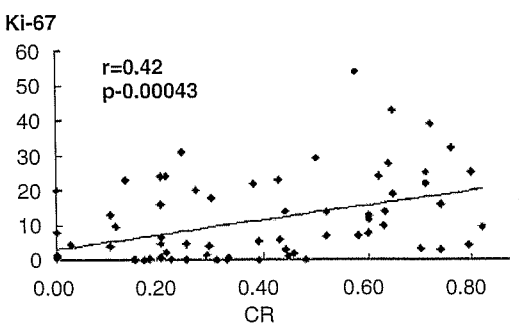

Figure 6. The correlation between CR values and Ki-67 staining scores in the 71 patients with clinical stage IA.: $r = 0.42$; $P = 0.00043$.

cerebellum showed significantly higher sensitivity than the SUV (19). We therefore used the CR value with contralateral lung in the present study.

The present study has demonstrated the following points: (i) tumors with high FDG uptake (CR ⩾ 0.55) could be identified as those at stages that are more advanced than stage IB with the sensitivity of 0.83 and the specificity of 0.81; (ii) FDG uptake and Ki-67 staining scores correlated with the pathological tumor stage and intratumoral invasiveness, although cyclin D1 and p53 did not show such correlation; and (iii) FDG uptake and Ki-67 scores were significantly correlated with each other.

Earlier reports have indicated that adenocarcinomas with GGO image are usually N0 stage and show low FDG uptake on PET (15,16,30). The present study is basically in agreement with these results, that is, adenocarcinomas with GGO image showed lower FDG uptake than those with solid one. However, one adenocarcinoma with GGO image was stage IB, which showed rather high CR than 25 stage IA tumors. In tumors with solid image, the 11 tumors with advanced stages showed significantly higher CR values than the 34 tumors with stage IA. Therefore, the FDG uptake on PET could be an independent factor for predicting pathological stage in clinical T1N0M0 lung adenocarcinomas.

It has been reported that 25% of clinical stage IA adenocarcinomas are pathologically advanced tumor stage (31). Recently, neoadjuvant chemotherapy has been reported to improve survival in clinical stages IB, II and IIIA of NSCLC (32). The present study showed that the CR value of 0.55 could be the cut-off value for predicting advanced tumor stages more than IB. Therefore, we propose that to improve patients' prognosis in clinical stage IA adenocarcinoma, mediastinoscopy or neoadjuvant chemotherapy should be performed for clinical stage IA adenocarcinoma with CR ⩾ 0.55.

The Ki-67 antigen exists in the nucleus of proliferating cells and has been reported to be a prognostic factor in lung cancer (1). Vesselle et al. (14) reported that the FDG uptake correlated with Ki-67 staining scores in 39 patients with NSCLC. They also described that the correlation between the FDG-uptake and Ki-67 staining scores was stronger in stage I than in stages I–III. Their report supported the present study, showing a significant correlation between the FDG uptake and Ki-67 staining scores in clinical stage IA lung adenocarcinomas.

Cyclin D1 is known to regulate the G_1-to-S phase transition during the cell cycle, and its expression in tumor cells is reported to correlate with their proliferative activity. However, several immunohistochemical studies on involvement of cyclin D1 in lung cancer had shown different results (2–5). While some authors reported the opposite finding, that is, the cyclin D1 staining scores was a predictor of poor prognosis of NSCLC (4,5), others have questioned its role as a predictor (3).

On the other hand, another report described that the negative staining for cyclin D1 correlated with poor prognosis (2). While these previous studies examined the expression of cyclin D1 in NSCLC including all histological types, the present study investigated the clinical stage IA adenocarcinomas, showing that cyclin D1 scores did not correlate with the FDG uptake, pathological tumor stage or tumor invasiveness. Our results indicate that Ki-67 is a better marker for the proliferative activity and malignant grade of adenocarcinomas than cyclin D1.

An alteration of p53 is reported to be a poor prognostic factor in many types of tumors including lung cancer (6), although one recent report has denied it (2). While Sasaki et al. (7) reported that the FDG uptake in tumors with the alteration of p53 tended to be higher than in those without, the present study did not find any correlation of p53 staining scores with the FDG uptake, tumor stage and intratumoral invasiveness in clinical stage IA lung adenocarcinomas. The differences between the report by Sasaki et al. and ours were (i) the number of the patients (28 versus 71 patients); (ii) histological types (NSCLC including all histological types versus adenocarcinoma); (iii) size of tumors (17,18) (no details about specific sizes versus 1–3 cm); (iv) measurement of FDG uptake (SUV versus CR). As described in our previous reports, the FDG uptake should be measured by CR and not by SUV, and should also be evaluated in adenocarcinomas with limited tumor size (16,19). Therefore, we believe that the alteration of p53 does not correlate with FDG uptake and therefore cannot be a dictator for the malignant grade in clinical stage IA lung adenocarcinomas.

We conclude that the FDG uptake can predict pathological tumor stage and tumor proliferative activity determined by Ki-67, but cannot predict the alteration of p53 in clinical stage IA lung adenocarcinomas. These results should be useful in determining the indication for mediastinoscopy or neoadjuvant chemotherapy in patients with clinical stage IA lung adenocarcinoma.

Acknowledgment

We thank technologists of the Nishidai Clinic who cooperated for the measurement of the CR value. We also thank laboratory technicians of the Department of Pathology of Saiseikai Central Hospital for supporting the immunohistochemical study.

References

1. Martin B, Paesmans M, Mascaux C, Berghmans T, Lothaire P, Meert A, et al. Ki-67 expression and patients survival in lung cancer: systematic review of the literature with meta-analysis. *Br J Cancer* 2004;91:2018–25
2. Au NH, Cheang M, Huntsman DG, Yorida E, Coldman A, Elliott WM, et al. Evaluation of immunohistochemical markers in non-small cell lung cancer by unsupervised hierarchical clustering analysis: a tissue microarray study of 284 cases and 18 markers. *J Pathol* 2004;204:101–9
3. Saitoh G, Sugio K, Ishida T, Sugimachi K. Prognostic significance of p21waf1, cyclin D1 and retinoblastoma expression detected by immunohistochemistry in non-small cell lung cancer. *Oncol Rep* 2001;8:737–43
4. Jin M, Inoue S, Umemura T, Moriya J, Arakawa M, Nagashima K, et al. Cyclin D1, p16 and retinoblastoma gene product expression as a predictor for prognosis in non-small cell lung cancer at stages I and II. *Lung Cancer* 2001;34:207–18.
5. Oshita F, Ito H, Ikehara M, Ohgane N, Hamanaka N, Nakayama H, et al. Prognostic impact of survivin, cyclin D1, integrin beta1, and VEGF in patients with small adenocarcinoma of stage I lung cancer. *Am J Clin Oncol* 2004; 27:425–8.
6. Mitsudomi T, Hamajima N, Ogawa M, Takahashi T. Prognostic significance of p53 alterations in patients with non-small cell lung cancer: a meta-analysis. *Clin Cancer Res* 2000;6:4055–63.
7. Sasaki M, Sugio K, Kuwabara Y, Koga H, Nakagawa M, Chen T, et al. Alterations of tumor suppressor genes (Rb, p16, p27 and p53) and an increased FDG uptake in lung cancer. *Ann Nucl Med* 2003;17:189–96.
8. Gould MK, Maclean CC, Kuschner WG, Rydzak CE, Owens DK. Accuracy of positron emission tomography for diagnosis of pulmonary nodules and mass lesions: a meta-analysis. *JAMA* 2001;285:914–24.
9. Marom EM, Sarvis S, Herndon JE II, Patz EF Jr. T1 lung cancers: sensitivity of diagnosis with fluorodeoxyglucose PET. *Radiology* 2002; 223:453–9.
10. Nomori H, Watanabe K, Ohtsuka T, Naruke T, Suemasu K, Uno K. The size of metastatic foci and lymph nodes yielding false-negative and false-positive lymph node staging with positron emission tomography in patients with lung cancer. *J Thorac Cardiovasc Surg* 2004;127:1087–92.
11. Ahuja V, Coleman RE, Herndon J, Patz EF Jr. The prognostic significance of fluorodeoxyglucose positron emission tomography imaging for patients with nonsmall cell lung carcinoma. *Cancer* 1998;83:918–24.
12. Vansteenkiste JF, Stroobants SG, Dupont PJ, De Leyn PR, Verbeken EK, Deneffe GJ, et al. Prognostic importance of the standardized uptake value on (18)F-fluoro-2-deoxy-glucose-positron emission tomography scan in non-small-cell lung cancer: an analysis of 125 cases. Leuven Lung Cancer Group. *J Clin Oncol* 1999;17:3201–6.
13. Higashi K, Ueda Y, Yagishita M, Arisaka Y, Sakurai A, Oguchi M, et al. FDG PET measurement of the proliferative potential of non-small cell lung cancer. *J Nucl Med* 2000;41:85–92.
14. Vesselle H, Schmidt RA, Pugsley JM, Li M, Kohlmyer SG, Vallires E, et al. Lung cancer proliferation correlates with [F-18]fluorodeoxyglucose uptake by positron emission tomography. *Clin Cancer Res* 2000;6:3837–44.
15. Nomori H, Watanabe K, Ohtsuka T, Naruke T, Suemasu K, Kobayashi T, et al. Fluorine 18-tagged fluorodeoxyglucose positron emission tomographic scanning to predict lymph node metastasis, invasiveness, or both, in clinical T1 N0 M0 lung adenocarcinoma. *J Thorac Cardiovasc Surg* 2004;128: 396–401.
16. Nomori H, Watanabe K, Ohtsuka T, Naruke T, Suemasu K, Uno K. Evaluation of F-18 fluorodeoxyglucose (FDG) PET scanning for pulmonary nodules less than 3 cm in diameter, with special reference to the CT images. *Lung Cancer* 2004;45:19–27.
17. Cremerius U, Fabry U, Neuerburg J, Zimny M, Osieka R, Buell U. Positron emission tomography with 18F-FDG to detect residual disease after therapy for malignant lymphoma. *Nucl Med Commun* 1998;19:1055–63.
18. Menda Y, Bushnell DL, Madsen MT, McLaughlin K, Kahn D, Kernstine KH. Evaluation of various corrections to the standardized uptake value for diagnosis of pulmonary malignancy. *Nucl Med Commun* 2001;22:1077–81.
19. Nomori H, Watanabe K, Ohtsuka T, Naurke T, Suemasu K, Uno K. Visual and semiquantitative analyses for F-18 fluorodeoxyglucose PET scanning in pulmonary nodules 1 cm to 3 cm in size. *Ann Thorac Surg* 2005;79:984–88; discussion 989.
20. Sobin LW, Wittekind CH. UICC TNM classification of malignant tumours. 6th edn. New York: Wiley-Liss 2002;131–41.
21. Moses LE, Shapiro D, Littenberg B. Combining independent studies of a diagnostic test into a summary ROC curve: data-analytic approaches and some additional considerations. *Stat Med* 1993;12:1293–316.
22. Allred DC, Harvey JM, Berardo M, Clark GM. Prognostic and predictive factors in breast cancer by immunohistochemical analysis. *Mod Pathol* 1998;11: 155–68.
23. Kim CK, Gupta NC, Chandramouli B, Alavi A. Standardized uptake values of FDG: body surface area correction is preferable to body weight correction. *J Nucl Med* 1994;35:164–7.
24. Lindholm P, Minn H, Leskinen-Kallio S, Bergman J, Ruotsalainen U, Joensuu H. Influence of the blood glucose concentration on FDG uptake in cancer—a PET study. *J Nucl Med* 1993;34:1–6.

25. Hamberg LM, Hunter GJ, Alpert NM, Choi NC, Babich JW, Fischman AJ. The dose uptake ratio as an index of glucose metabolism: useful parameter or oversimplification? *J Nucl Med* 1994;35:1308–12.
26. Dewan NA, Gupta NC, Redepenning LS, Phalen JJ, Frick MP. Diagnostic efficacy of PET-FDG imaging in solitary pulmonary nodules. Potential role in evaluation and management. *Chest* 1993;104:997–1002.
27. Gupta NC, Maloof J, Gunel E. Probability of malignancy in solitary pulmonary nodules using fluorine-18-FDG and PET. *J Nucl Med* 1996;37:943–8.
28. Imdahl A, Jenkner S, Brink I, Nitzsche E, Stoelben E, Moser E, et al. Validation of FDG positron emission tomography for differentiation of unknown pulmonary lesions. *Eur J Cardiothorac Surg* 2001;20:324–9.
29. Lowe VJ, Fletcher JW, Gobar L, Lawson M, Kirchner P, Valk P, et al. Prospective investigation of positron emission tomography in lung nodules. *J Clin Oncol* 1998;16:1075–84.
30. Nomori H, Ohtsuka T, Naruke T, Suemasu K. Histogram analysis of computed tomography numbers of clinical T1N0M0 lung adenocarcinoma with special reference to lymph node metastasis and tumor invasiveness. *J Thorac Cardiovasc Surg* 2003;126: 1584–9.
31. Asamura H, Nakayama H, Kondo H, Tsuchiya R, Shimosato Y, Naruke T. Lymph node involvement, recurrence, and prognosis in resected small, peripheral, non-small-cell lung carcinomas: are these carcinomas candidates for video-assisted lobectomy? *J Thorac Cardiovasc Surg* 1996;111:1125–34.
32. Depierre A, Milleron B, Moro-Sibilot D, Chevret S, Quoix E, Lebeau B, et al. Preoperative chemotherapy followed by surgery compared with primary surgery in resectable stage I (except T1N0), II, and IIIa non-small-cell lung cancer. *J Clin Oncol* 2002;20:247–53.

Jpn J Clin Oncol 2006;36(11)694–698
doi:10.1093/jjco/hyl092

Characteristics of Advantages of Positron Emission Tomography over Computed Tomography for N-staging in Lung Cancer Patients

Akinori Ebihara[1], Hiroaki Nomori[2,3], Kenichi Watanabe[2], Takashi Ohtsuka[2], Tsuguo Naruke[2], Kimiichi Uno[4], Ichiro Kuwahira[5] and Kenji Eguchi[5]

[1]Department of Internal Medicine, Saiseikai Central Hospital, Tokyo, [2]Department of Thoracic Surgery, Saiseikai Central Hospital, Tokyo, [3]Department of Thoracic Surgery, Graduate School of Medical and Pharmaceutical Sciences, Kumamoto University, Kumamoto, [4]Nishidai Clinic, Tokyo and [5]Department of Internal Medicine, Tokai University School of Medicine, Isehara, Kanagawa, Japan

Received March 2, 2006; accepted July 16, 2006; published online October 26, 2006

Objective: We analyzed the characteristics of advantages of positron emission tomography (PET) over computed tomography (CT) for N-staging in lung cancer patients.
Methods: Preoperative PET and CT scans were performed for 2057 lymph node stations in 205 patients with peripheral-type lung cancer. The advantages of PET over CT for N-staging were analyzed among lymph node locations and histological subtypes.
Results: The pathological N-stages were N0 in 143 patients, N1 in 31, N2 in 24 and N3 in 7. PET was able to diagnose N0, N2 and N3 diseases more accurately than CT ($P = 0.03$, 0.01 and 0.02, respectively), but there was no significant difference between the two modalities for N1 disease. In the upper mediastinal lymph node stations, both false-negative and false-positive were significantly less frequent with PET than with CT ($P = 0.001$). In the lower mediastinal and supra clavicle lymph nodes, PET showed a lower frequency of false-negative than CT ($P = 0.04$ and 0.003, respectively), but there was no significant difference in the frequency of false-positive between the two modalities. Among histological types, PET could stage adenocarcinoma with less frequent false-negative and squamous cell carcinoma with less frequent false-positive than CT ($P = 0.02$ and 0.005, respectively).
Conclusion: For N-staging, PET was superior to CT for the following: (1) more accurate for N0, N2 and N3 diseases but not for N1; (2) lower frequency of false-positive in the upper mediastinal nodes; and (3) lower frequencies of false-negative in adenocarcinoma and false-positive in squamous cell carcinoma. Recognizing these advantages of PET could make the N-staging of lung cancer more accurate.

Key words: positron emission tomography – computed tomography – lymph node stage – lung cancer – adenocarcinoma

INTRODUCTION

CT scanning has been a usual procedure of N-staging of lung cancer. However, CT scanning is not sufficiently sensitive or specific for diagnosing lymph node metastasis, because size is the only criterion used to differentiate benign from malignant lymph nodes (1). In recent years, ^{18}F-fluorodeoxyglucose (FDG)-PET scanning has been used for the staging of lung cancer (2–7). Because of the biological nature of FDG, FDG-PET has been reported to be able to detect metastatic lymph nodes more accurately than CT. A meta-analysis by Dwamena et al. of PET scanning of 514 patients in 14 studies showed that the mean sensitivity and specificity of PET scanning for N-staging were 0.79 (range: 0.62–0.97) and 0.91 (range: 0.79–0.99), respectively, both being superior to those of CT scanning, i.e. 0.60 (range: 0.25–0.89) and 0.77 (range: 0.44–0.95) (1). However, the advantages of PET over CT for lymph node staging of lung cancers have not been fully characterized. In this study we examined the characteristics of advantages of PET over CT for lymph node staging, especially among various lymph node locations and histological types.

For reprints and all correspondence: Hiroaki Nomori, Department of Thoracic Surgery, Graduate School of Medical Sciences, Kumamoto University, 1-1-1, Honjo, Kumamoto 860-8556, Japan. E-mail: hnomori@kaiju.medic.kumamoto-u.ac.jp

PATIENTS AND METHODS

Subjects

Between December 2001 and March 2005, 205 patients with peripheral lung cancer more than 1 cm in size prospectively underwent FDG-PET and CT scanning during the month before surgery. A total of 2057 lymph node stations in these 205 patients were evaluated. The histological type of lung cancer was adenocarcinoma in 151 patients, squamous cell carcinoma in 37, large cell carcinoma in eight, small cell carcinoma in two, adenosquamous carcinoma in four, carcinosarcoma in two and atypical carcinbid in one (Table 1). The histological criteria were based on the 1999 World Health Organization classification (8). The pathological N stages were N0 in 143, N1 in 31, N2 in 24 and N3 in seven. The classification of lymph nodes was done according to the original lymph node map of lung cancer (9). All patients underwent pneumonectomy, lobectomy, or segmentectomy with mediastinal lymph node dissection, except for seven patients with clinical N3 disease in whom pathological N-stages were evaluated by mediastinoscopy and/or scalene node biopsy.

FDG-PET Scanning

Patients were instructed to fast for at least 4 h prior to intravenous (IV) administration of ^{18}F-FDG. The administered dosage of ^{18}F-FDG was 125 μCi/kg (4.6 MBq/kg) for non-diabetic patients and 150 μCi/kg (5.6 MBq/kg) for diabetic patients. PET imaging was performed approximately 60 min after administration of the FDG with a POSICAM.HZL m-POWER (Positron Co., Houston, Texas, USA). Initially no attenuation-corrected emission scans were obtained during the two-dimensional, high-sensitivity mode for 4 min per bed position, taken from the vertical-skull through the mid-thighs. Immediately thereafter, a two-bed-position attenuation-corrected examination was performed with 6 min for the emission sequence and 6 min for the transmission sequence at each bed position. The images were usually reconstructed in a 256 × 256 matrix by using ordered subset expectation maximization corresponding to a pixel size of 4 × 4 mm, with section spacing of 2.66 mm.

Table 1. Characteristics of patients

Variable	Data
Age (years)	67 ± 19
Sex	
Male	134
Female	71
Tumor size (cm)	3.0 ± 1.8
Histology	
Adenocarcinoma	151
Squamous cell carcinoma	37
Large cell carcinoma	8
Small cell carcinoma	2
Adenosquamous carcinoma	4
Carcinosarcoma	2
Atypical carcinoid	1
Pathological N stage	
N0	143
N1	31
N2	24
N3	7
Total	205

N Staging by PET Scanning

PET data were evaluated visually and/or semi-quantitatively. Based on visual findings, the lymph nodes showing clearly greater or less FDG-uptake than the mediastinal blood pool were diagnosed as positive and negative, respectively. Two examiners (A.E. and K.U.), who were blinded for the pathological N-stage, evaluated the visual findings of PET. For the lymph nodes showing similar FDG-uptake to the mediastinal blood pool or where there was disagreement between the two examiners, semi-quantitative analysis was used as reported previously (10). Briefly, the regions of interest (ROIs) were placed in the lymph nodes and cerebellum. The highest activities in both the lymph node ROI (L) and the cerebellum ROI (C) were measured. The contrast ratio (CR) was calculated by L/C in each lymph node as an index of FDG uptake. The cut-off value was determined as 0.25, i.e. lymph nodes with CR $\geq$ 0.25 were defined as positive and those with CR $<$ 0.25 as negative.

N Staging by CT Scanning

Spiral CT was performed using a ProSeed SA (General Electric Medical System, Milwaukee, USA). The following acquisition parameters were used: high voltage (120 kV), tube load 160 mA, window level −500 Hounsfield units (HU) and window width 1500 HU. The entire thorax was scanned with 0.5 or 1-cm thick sections at 1 breath hold with maximum inspiration. The criterion of CT definition for suspected metastasis of the lymph node was a short-axis diameter of 1.0 cm or larger. Enhanced CT was additionally conducted for patients with CT-negative and PET-positive lymph nodes. The same two examiners for N-staging by PET evaluated the CT findings. For lymph nodes showing disagreement between the two examiners, N-sages were determined after their discussion.

Statistical Analysis

True-positive (TP), true-negative (TN), false-positive (FP) and false-negative (FN) results of PET and CT scanning for lymph node metastasis were compared with the results of pathological diagnosis. Sensitivity was calculated as TP/TP + FN, specificity as TN/TN + FP, positive predictive

value as TP/TP + FP, negative predictive value as TN/TN + FN and accuracy as TP + TN/Total. The advantages of PET over CT were evaluated for each pathological N-stage, lymph node location and each histological type. All data were analyzed for significance by using the Stat View software χ^2 test. Differences at $P < 0.05$ were accepted as significant. All values in the text and tables are given as mean ± SD.

RESULTS

Table 2 shows the correlation between the N-staging by PET and CT and pathological N-stage. PET was able to diagnose N0, N2 and N3 diseases more accurately than CT with significant difference ($P = 0.03$, 0.01 and 0.02, respectively). However, there was no difference between PET and CT in the accuracy in diagnosing N1 disease ($P = 0.4$).

Of the 2057 lymph node stations examined, 15 showed similar FDG-uptake to the mediastinal blood pool. Of those 15 lymph nodes, six showed CR ≥ 0.25 (positive) and the remaining nine showed CR < 0.25 (negative). PET scanning yielded TP in 85 lymph node stations, FN in 46, FP in 11 and TN in 1915 (Table 3). For the same lymph node stations, CT scanning yielded TP in 49 lymph node stations, FN in 82, FP in 22 and TN in 1904. As a result, the sensitivity of PET was 0.65, which was significantly higher than 0.37 of CT ($P < 0.0001$). The positive predictive value of PET was 0.89, which was significantly higher than 0.7 of CT ($P = 0.02$). However, there was no significant difference in specificity, accuracy and negative predictive value between the two diagnostic modalities.

The locations of FP lymph node stations revealed by PET and CT are shown in Table 4. Of the 670 upper mediastinal lymph node stations without metastasis, PET showed FP less frequently than CT ($P = 0.001$). One FP upper mediastinal lymph node, demonstrated by PET was Botallo's lymph node, showed lymphadenitis probably as a result of tuberculosis accompanying the adenocarcinoma. The other locations of FP lymph nodes did not show any difference between PET and CT.

Table 2. Coincidence of N-staging by PET and CT with pathological N-stage

Pathological N-stage	No. of coincidences with pathological N-stage		Difference
	PET	CT	
N0 ($n = 143$)	138	129	$P = 0.03$
N1 ($n = 31$)	19	16	NS
N2 ($n = 24$)	16	7	$P = 0.01$
N3 ($n = 7$)	7	3	$P = 0.02$

PET, positron emission tomography; CT, computed tomography; NS, not significant.

The locations of FN lymph node stations revealed by PET and CT are shown in Table 5. For the upper mediastinal, lower mediastinal and supra-clavicle lymph nodes with metastasis, PET showed FN less frequently than CT ($P = 0.001$, 0.04 and 0.003). However, for hilar lymph nodes, there was no significant difference of FN between PET and CT.

The difference of histological types in patients who were understaged or overstaged by PET and CT are shown in Tables 6 and 7. For adenocarcinoma, PET showed significantly less understaging than CT ($P = 0.02$) (Table 6). For squamous cell carcinoma, PET showed significantly less overstaging than CT (Table 7) ($P = 0.005$). All seven squamous cell carcinoma patients who were overstaged by CT were heavy smokers, whose Brinkman Index was 680–2400 (mean ± SD: 1444 ± 525).

DISCUSSION

Several criteria have been used to detect lymph node metastases of lung cancer using PET scanning, including accumulation of FDG without objective criteria (6, 11),

Table 3. PET and CT analyses with pathological diagnosis

Diagnosis	No. of lymph node stations		Total
	With metastasis	Without metastasis	
PET			
Positive	85	11	96
Negative	45	1915	1961
CT			
Positive	49	22	71
Negative	82	1904	1986
Total	131	1926	2057

PET, positron emission tomography; CT, computed tomography.

Table 4. False positive lymph node stations with PET and CT

Locations of LNS	No. of LNS without metastasis	False positive with		Difference
		PET	CT	
Upper mediastinum	670	1	12	$P = 0.001$
Lower mediastinum	510	4	3	NS
Hilar	745	4	7	NS
SCN	1	1	0	NS
Total	1926	10	22	

PET, positron emission tomography; CT, computed tomography; LNS, lymph node station; SCN, supra clavicle lymph node; NS, not significant.

Table 5. False negative lymph node stations with PET and CT

Locations of LNS	No. of LNS without metastasis	False positive with		Difference
		PET	CT	
Upper mediastinum	47	14	30	$P = 0.001$
Lower mediastinum	8	2	6	$P = 0.04$
Hilar	70	30	40	$P = 0.1$
SCN	6	1	6	$P = 0.003$
Total	128	45	82	

PET, positron emission tomography; CT, computed tomography; LNS, lymph node station; SCN, supra clavicle lymph node.

Table 6. Difference of histological types whose N-stages were understaged by PET and CT

Histological type	No. of patients	Understaging by	
		PET	CT
Adenocarcinomas	151	11	24*
Non-adenocarcinomas	54	8	13
Total	205	19	37

PET, positron emission tomography; CT, computed tomography.
*Adenocarcinomas are more frequently understaged by CT than by PET ($I = 0.02$).

accumulation greater than mediastinal blood flow (2–4), and CR with the paravertebral muscles (12). We evaluated the lymph nodes with similar FDG-uptake to mediastinal blood pool by using the activity ratio in comparison to the cerebellum, as reported previously (10), because accumulation of FDG in the cerebellum was more stable than that in mediastinal blood flow or muscle.

While several authors have reported the superiority of PET over CT for N-staging of lung cancer (1–7), the present study showed that PET was able to identify N0, N2 and N3 diseases significantly more accurately than CT. However, there was no difference between the two modalities for N1 disease. These results appeared to be supported by data obtained by Vesselle et al., who reported that PET scanning could not reliably identify N1 disease, with only 6 of 21 cases identified (13).

It is well known that the inflammatory condition of lymph nodes can cause FP results of FDG-PET in lung cancer. Takamochi et al. reported that 10 of 71 patients (14%) with NSCLC showed FP lymph nodes with PET (14). While they did not show the location of the FP lymph nodes, the present study demonstrated that PET showed a lower frequency of FP in the upper mediastinal lymph nodes than CT. Thus we concluded that PET-positive lymph nodes in the upper

Table 7. Difference of histological types whose N-stages were overstaged with PET and CT

Histological type	No. of patients	Overstaging by	
		PET	CT
Squamous cell carcinomas	37	0	7*
Non-squamous cell carcinomas	168	5	12
Total	205	5	19

PET, positron emission tomography; CT, computed tomography.
*Squamous cell carcinomas are more frequently overstaged by CT than by PET ($P = 0.005$).

mediastinum could be truly positive for metastasis, making it possible to reduce the need of mediastinoscopy in such patients. However, because there was some possibility of FP in the lower mediastinum and hilar nodes, transbronchial needle or thoracoscopic biopsy is recommended for these regions.

In the analysis of histological types, the present study showed that PET was able to reduce the incidences of FN in adenocarcinoma and FP in squamous cell carcinoma in comparison with CT. Ohta et al. reported that nodal micrometastasis was detected by immunohistochemistry in 20% of patients with adenocarcinoma 1–2 cm in size, whereas it was not found in any patients with squamous cell carcinoma of the same size (15). Mori et al. reported that lymph node metastases from adenocarcinoma frequently showed normal size, resulting in lower sensitivity of N-staging by CT than those from squamous cell carcinoma (16). They also reported that CT scanning showed FP lymph nodes more frequently in squamous cell carcinoma than in adenocarcinoma (16). Because the present study examined peripheral-type lung cancer, there were no enlarged lymph nodes caused by inflammation, such as obstructive pneumonia and atelectasis. Because all seven patients with squamous cell carcinoma whose N-stages were overstaged by CT smoked heavily, the enlarged lymph nodes could be caused by smoking.

We conclude that PET is more advantageous for lymph node staging than CT. However, the advantage depends on the lymph node locations and histological types. Realizing the characteristic advantages of PET is useful for accurate lymph node staging in lung cancer.

References

1. Dwamena BA, Sonnad SS, Angobaldo JO, Wahl RL. Metastases from non-small cell lung cancer: mediastinal staging in the 1990s – meta-analytic comparison of PET and CT. *Radiology* 1999;213:530–6.
2. Gupta NC, Tamin WJ, Graeber GG, Bishop HA, Hobbs GR. Mediastinal lymph node sampling following positron emission tomography with fluorodeoxyglucose imaging in lung cancer staging. *Chest* 2001;120:521–7.
3. Gupta NC, Graeber GM, Bishop HA. Comparative efficacy of positron emission tomography with fluorodeoxyglucose in evaluation of small (<1 cm), intermediate (1 to 3 cm), and large (>3 cm) lymph node lesions. *Chest* 2000;117:773–8.

4. Graeter TP, Hellwig D, Hoffman K, Ukena D, Kirsch CM, Schafers HJ. Mediastinal lymph node staging in suspected lung cancer: comparison of positron emission tomography with F-18-fluorodeoxyglucose and mediastinoscopy. *Ann Thorac Surg* 2003;75:231–6.
5. Chin R Jr, Ward R, Keyes JW, Choplin RH, Reed JC, Wallenhaupt S, et al. Mediastinal staging of non-small cell lung cancer with positron emission tomography. *Am J Respir Crit Care Med* 1995;152:2090–6.
6. Bury T, Paulus P, Dowlati A, Corhay JL, Weber T, Ghaye B, et al. Staging of the mediastinum: value of positron emission tomography imaging in non-small cell lung cancer. *Eur Respir J* 1996;9:2560–4.
7. Valk PE, Pounds TR, Hopkins DM, Haseman MK, Hofer GA, Greiss HB, et al. Staging non-small cell lung cancer by whole-body positron emission tomography imaging. *Ann Thorac Surg* 1995;60:1573–82.
8. Travis WE, Colby TV, Corrin B, Shimosato Y, Brambilla E. World Health Organization international histological classification of tumours. Histological typing of lung and pleural tumours. 3rd edn. (In collaboration with LH Sobin and pathologists from 14 countries). Berlin: Springer; 1999.
9. Naruke T, Suemasu K, Ishikawa S. Lymph node mapping and curability at various levels of metastasis in resected lung cancer. *J Thorac Cardiovasc Surg* 1978:832–9.
10. Nomori H, Watanabe K, Ohtsuka T, Naruke T, Suemasu K, Uno K. The size of metastatic foci and lymph nodes yielding false-negative and false-positive lymph node staging with positron emission tomography in patients with lung cancer. *J Thorac Cardiovasc Surg* 2004;127:1087–92.
11. Lowe VJ, Fletcher JW, Gobar L, Lawson M, Kirchner P, Valk P, et al. Prospective investigation of positron emission tomography in lung nodules. *J Clin Oncol* 1998;16:1075–84.
12. Yasukawa T, Yoshikawa K, Aoyagi H, Yamamoto N, Tamura K, Suzuki K, et al. Usefulness of PET with ^{11}C-Methionine for the detection of hilar and mediastinal lymph node metastasis in lung cancer. *J Nucl Med* 2000;41:283–90.
13. Vesselle H, Pugsley JM, Vallieres E, Wood DE. The impact of fluorodeoxyglucose F 18 positron-emission tomography on the surgical staging of non-small cell lung cancer. *J Thorac Cardiovasc Surg* 2002;124:511–9.
14. Takamochi K, Yoshida J, Murakami K, Niho S, Ishii G, Nishimura M, et al. Pitfalls in lymph node staging with positron emission tomography in non-small cell lung cancer patients. *Lung Cancer* 2005;47:235–42.
15. Ohta Y, Oda M, Wu J, Tsunezuka Y, Hiroshi M, Nomura A, et al. Can tumor size be guide for limited surgical intervention in patients with peripheral non-small cell lung cancer? *J Thorac Cardiovasc Surg* 2001;122:900–6.
16. Mori K, Yokoi K, Saito Y, Tominaga K, Miyazawa N. Diagnosis of mediastinal lymph node metastases in lung cancer. *Jpn J Clin Oncol* 1992;22:35–40.

Sentinel node navigation segmentectomy for clinical stage IA non–small cell lung cancer

Hiroaki Nomori, MD, PhD,[a] Koei Ikeda, MD, PhD,[a] Takeshi Mori, MD,[a] Hironori Kobayashi, MD,[a] Kazunori Iwatani, MD,[a] Koichi Kawanaka, MD, PhD,[b] Shinya Shiraishi, MD, PhD,[b] and Toshiaki Kobayashi, MD, PhD[c]

From right to left: Drs Nomori, Mori, and Ikeda. The Bronze statue is Dr Shibasaburo Kitasato

Objective: Intraoperative frozen section examination of sentinel lymph nodes was conducted to determine the final indication for segmentectomy for clinical T1 N0 M0 non–small cell lung cancer.

Methods: Between April 2005 and July 2006, 52 patients with clinical T1 N0 M0 non–small cell lung cancer were prospectively treated by segmentectomy with sentinel node identification. The day before surgery, technetium-99m tin colloid was injected into the peritumoral region. After segmentectomy and lymph node dissection, sentinel nodes identified by measuring radioactive tracer uptake were examined for intraoperative frozen sections, which were serially cut 2 to 3 mm in thickness. When sentinel node metastasis was observed, segmentectomy was converted to lobectomy.

Results: Sentinel nodes were identified in 43 (83%) patients. The average number of sentinel nodes was 1.6 ± 0.9 (range: 1–5) per patient. Of 3 patients with metastatic sentinel lymph nodes, 2 underwent lobectomy and 1 larger segmentectomy. None of the other 40 patients had metastatic sentinel lymph nodes and therefore they were treated with segmentectomy. Pathologic staging with permanent sections was N0 in all of the 40 patients. On the other hand, in 9 patients whose sentinel nodes could not be identified, intraoperative frozen sections were required for 5.4 ± 2.3 lymph nodes, which was significantly more than 1.6 ± 0.9 in the 43 patients with sentinel node identification ($P < .001$).

Conclusion: Sentinel node identification is useful to determine the final indication of segmentectomy for clinical T1 N0 M0 non–small cell lung cancer by targeting the lymph nodes needed for intraoperative frozen section diagnosis.

From the Departments of Thoracic Surgery[a] and Radiology,[b] Graduate School of Medical Sciences, Kumamoto University, Honjo, Kumamoto, Japan; and the Department of Assistive Diagnostic Technology,[c] National Cancer Center Hospital, Tokyo, Japan.

This work was supported, in part, by Grant-in-Aid from the Ministry of Health, Labor, and Welfare, Japan.

Received for publication Aug 20, 2006; revisions received Oct 7, 2006; accepted for publication Oct 23, 2006.

Address for reprints: Hiroaki Nomori, MD, PhD, Department of Thoracic Surgery, Graduate School of Medical Sciences, Kumamoto University, 1-1-1 Honjo, Kumamoto 860-8556, Japan (E-mail: hnomori@qk9.so-net.ne.jp).

J Thorac Cardiovasc Surg 2007;133:780-5

0022-5223/$32.00

doi:10.1016/j.jtcvs.2006.10.027

GTS

In 1995, the Lung Cancer Study Group[1] conducted a prospective randomized controlled trial of limited resection versus lobectomy for clinical T1 N0 M0 non–small cell lung cancer (NSCLC) and concluded that the former was inferior to the latter regarding local recurrence and survival. However, the limited resection group in the study included both segmentectomy and wedge resection, and the curability for T1 N0 M0 NSCLC differed between the two procedures. On the other hand, there have been several reports describing that survivals were similar between patients treated with segmentectomy and those with lobectomy.[2-7]

The most important issue regarding segmentectomy versus lobectomy is whether postoperative local recurrence is increased. Whereas Warren and Faber[8] reported local recurrence in 15 (22.7%) of 66 patients after segmentectomy versus 5 (4.9%) of 103 patients after lobectomy, other authors reported that local recurrence after segmentectomy with complete dissection of hilar and mediastinal lymph nodes was equal to that after lobectomy.[3-6] However, for determining the final indication for segmentectomy, intraoperative frozen sections must be examined for all of the hilar

Abbreviations and Acronyms
CT = computed tomography
FDG-PET = fluorodeoxyglucose–positron emission tomography
NSCLC = non–small cell lung cancer
SN = sentinel node
SPECT = single photon emission computed tomography

and lobe-specific mediastinal lymph nodes to confirm the intraoperative N staging to be N0.[3-6]

A sentinel node (SN) is defined as the first lymph node within the lymphatic basin reached by lymph draining from the primary lesion. Recently, SNs have been identified by a radioactive tracer with or without dye during surgery for melanoma, breast cancer, gastrointestinal cancer, and lung cancer to reduce lymph node dissection.[9-14] We[13,14] previously reported that SN identification with technetium-99m tin colloid could establish the first site of nodal metastasis in NSCLC.

In the present study, we used SN identification to target the lymph nodes submitted for intraoperative frozen section diagnosis, which might determine the indication of segmentectomy. In addition, unlike Tsubota,[3] Okada,[4] Yoshikawa,[5] and their associates, who proposed that the indication for segmentectomy was T1 N0 M0 NSCLC less than 2 cm in size, we proposed that it was T1 N0 M0 NSCLC without size limitation. Because SN identification served as the final indication of segmentectomy, we named the procedure "sentinel node navigation segmentectomy."

Patients and Methods

Eligibility

The study protocol for SN navigation segmentectomy was approved by the Ethics Committee of Kumamoto University Hospital in March 2005. Informed consent was obtained from all patients after discussing the risks and benefits of the proposed surgery with their surgeons.

Patients

Between April 2005 and July 2006, 103 patients with NSCLC underwent surgical treatment. Of these, 73 patients had stage c-T1 N0 M0 cancer according to the findings of both computed tomography (CT) and fluorodeoxyglucose–positron emission tomography (FDG-PET). SN navigation segmentectomy was prospectively performed when (1) c-T1 N0 M0 NSCLC was identified in the peripheral lung; (2) the tumor on CT was more than 2 cm away from the pulmonary vein running at the boundary of the affected segment; (3) intraoperative frozen sections of SN showed no metastasis; (4) the surgical margin was intraoperatively found to be more than 2 cm from the tumor; and (5) tumors located centrally within the inner one third of the lung or in the right middle lobe were excluded. The stage of disease was based on the TNM classification of the International Union Against Cancer.[15] The lymph node nomenclature used was according to the lymph node map of Naruke and associates,[16] which was approved by the Japan Lung Cancer Society (Table 1).

TABLE 1. Lymph node nomenclature

N2 node	N1 node
Superior mediastinal	Hilar
No. 1. Highest mediastinal	No. 10. Hilar
No. 2. Paratracheal	No. 11. Interlobar
No. 3. Pretracheal	No. 12. Lobar
No. 4. Tracheobronchial	
Aortic	Intrapulmonary
No. 5. Botallo	No. 13. Segmental
No. 6. Para-aortic	No. 14. Subsegmental
Inferior mediastinal	
No. 7. Subcarinal	
No. 8. Paraesophageal	
No. 9. Pulmonary ligament	

Administration of Radioactive Colloid

The day before surgery, a 23-gauge needle was introduced into the peritumoral region under single photon emission computed tomography/computed tomography (SPECT/CT) system guidance, which incorporates a gantry-free SPECT with dual-head detectors (Skylight; ADAC Laboratories, Milpitas, Calif) and an 8 multidetector CT scanner (Light-Speed Ultra; General Electrics, Milwaukee, Wis). Technetium tin colloid (6−8 mCi) suspended in a 1- to 1.5-mL volume was injected in a single shot. SPECT/CT was performed 5 minutes after the injection and the next morning just before the operation.

SN Identification

The radioactivity of the resected lymph nodes was counted with a handheld gamma probe (Navigator; Auto Suture Japan, Tokyo, Japan). The radioactivity was measured for a 10-second period. SN was defined as any node for which the count was more than 5 times the radioactivity of the resected tissue with the lowest count.

SN Navigation Segmentectomy

Under thoracotomy, SN navigation segmentectomy was performed as follows: (1) Pulmonary arteries and bronchi of the affected segments were cut at the hilum; (2) pulmonary veins along the boundary of segments were isolated from the center to periphery; (3) the affected segments along the pulmonary veins were resected with staplers; (4) the hilar and systematic mediastinal lymph nodes were dissected; (5) the radioactivity of dissected lymph nodes was counted for SN identification; (6) SNs were examined by intraoperative frozen sections, which were serially cut 2 to 3 mm in thickness; (7) if the intraoperative frozen sections of the SN showed no metastasis, the operation was completed with segmentectomy; (8) if the sections of the SN showed metastasis, lobectomy was performed; and (9) if the SN could not be identified because radioactivity of the lymph nodes was low, all of the hilar and lobe-specific mediastinal lymph nodes were submitted for

GTS

TABLE 2. Sites of segmentectomy

Segment	No. of patients	Segment	No. of patients
Right		Left	
Upper lobe		Upper lobe	
S1	3	S1 + 2	4
S2	2	S3	2
S1 + S2	2	S1 + 2 + 3	9
S3	2	S4 + 5	7
S3 + S2b	1		
S2 + S3a	1		
Lower lobe		Lower lobe	
S6	4	S6	3
S7 + 8	1	S8	1
S8	1	S8 + 9	2
S9 + S10	2	S9 + 10	1
S7–10	1	S10	1
S6 + S9 + S10	1	S8–10	1
Total	21		31

Right upper lobe: *S1*, apical; *S2*, anterior; *S3*, posterior. Right lower lobe: *S6*, apical; *S7*, medial; *S8*, anterior; *S9*, lateral; *S10*, posterior. Left upper lobe: *S1+2*, apical posterior; *S3*, apical anterior; *S4*, superior lingular; *S5*, inferior lingular. Left lower lobe: *S6*, apical; *S8*, anterior; *S9*, lateral; *S10*, posterior.

TABLE 3. Characteristics of patients with and without sentinel node identification

	Sentinel lymph node	
	Identifiable	Nonidentifiable
Mean age (y)	69 ± 7	71 ± 7
Sex		
Male	26	8
Female	17	1
Mean tumor size (cm)	1.9 ± 0.7	2.1 ± 0.7
Histologic type		
Adenocarcinoma	37	6
Squamous cell carcinoma	4	2
Adenosquamous carcinoma	2	1
No. of lymph nodes submitted for intraoperative frozen diagnosis	1.6 ± 0.9	5.4 ± 2.3*
Pathologic TNM		
T1 N0 M0	39	9
T2 N0 M0	1	0
T1 N1 M0	1	0
T2 N1 M0	1	0
T1 N2 M0	1	0
Total	43	9

*$P < .001$.

intraoperative frozen section. Lobe-specific lymph nodes were defined as follows: No. 3 and No. 4 for the right upper lobe, No. 5 for the left upper lobe, and No. 7 for the lower lobe of both sides.[17]

Primary End Points of the Study

Primary end points of the study are as follows: (1) Can SN identification diagnose pathologic N stage during segmentectomy? (2) Are the survival and local recurrence after SN navigation segmentectomy similar to those after lobectomy?

Statistical Analysis

All data were analyzed for significance by the 2-tailed Student *t* tests. All values in the text and tables are given as mean ± SD.

Results

Operative procedures for the 73 patients with c-T1 N0 M0 were lobectomy in 12 patients, segmentectomy in 52, and wedge resection in 9. The reasons for conducting lobectomy in the 12 patients were as follows: (1) tumors in the right middle lobe in 5 patients; (2) tumors located centrally in 5 patients; (3) multiple lesions in the same lobe in 1 patient; and (4) thoracoscopic lobectomy as requested by the patient. As a result, 52 patients were consecutively enrolled for SN navigation segmentectomy. Table 2 shows the sites of segmentectomy for the 52 patients. The average number of dissected lymph node stations and lymph nodes per patient was 6 ± 1.8 stations and 12.5 ± 5.9 lymph nodes, respectively. Among the 52 patients, SNs could be identified in 43 (83%). The time needed for SN identification was within 5 minutes in each patient. The characteristics of the 43 patients with SN identification and of the 9 patients without are shown in Table 3. Average tumor size on CT was 1.9 ± 0.7 cm (range: 0.8–3.0 cm) and 2.1 ± 0.7 cm (range: 1.4–3.0 cm) in the patients with and without SN identification, respectively. Seventeen (40%) of the 43 patients with SN identification and 4 (44%) of 9 patients without had tumors larger than 2 cm. Pathologic tumor stages in the 43 patients with SN identification were T1 N0 M0 in 39, T2 N0 M0 in 1, T1 N1 M0 in 1, T2 N1 M0 in 1, and T1 N2 M0 in 1, whereas the stage in all 9 patients without SN identification was p-T1 N0 M0. The tumors in 2 patients were pathologically classified as T2; one tumor was spread over the pleura and the other was more than 3 cm in size in the permanent section. The average number of lymph nodes submitted for intraoperative frozen section examination was significantly less in the 43 patients with SN identification (1.6 ± 0.9 [range: 1–5] per patient) than in the 9 patients without SN identification (5.4 ± 2.3 [range: 3–10] per patient) ($P < .001$).

Table 4 shows the SN identified in the hilar lymph node stations. The number of stations having SN increased in numeric order from No. 10 to 13 stations. In the mediastinal lymph node stations, the SN was identified in 15 of the 43 patients (35%). Eleven of the 15 patients had SNs in both the hilar and mediastinal lymph node stations, whereas the remaining 4 patients had SNs only in the mediastinum. The distribution of mediastinal SNs is shown in Table 5, which

TABLE 4. Sentinel lymph node mapping in the hilar lymph node stations

Station	Sentinel nodes	
	No. of patients	Percent
10	7/3	16.3
11	7/43	16.3
12	12/43	27.9
13	22/43	51.2

TABLE 5. Sentinel nodes at the mediastinum in each lobe

Tumor location	Station of mediastinal SN	No. of patients	Percent
RUL	3 or 4	3/10	30.0
RLL	3 or 4	2/9	22.2
	7 and 3	1/9	11.2
LUL	5	8/18	44.4
LLL	7	2/6	33.3

SN, Sentinel node; *RUL*, right upper lobe; *RLL*, right lower lobe; *LUL*, left upper lobe; *LLL*, left lower lobe.

was lobe-specific; that is, 3 of the 10 patients with primary tumor in the right upper lobe had SN in No. 3 or 4 stations; 3 of the 9 patients with primary tumor in the right lower lobe had SN in No. 7, 3, or 4 stations; 8 of the 18 patients with primary tumor in the left upper lobe had SN in No. 5 station; and 2 of the 6 patients with primary tumor in the left lower lobe had SN in No. 7 station.

In 3 (7%) of the 43 patients with SN identification, metastasis was found in the SN by intraoperative frozen section (Table 6). For 2 of the 3 patients (patients 1 and 2), operative procedures were converted to lobectomy. The operative procedure for the remaining patient (patient 3) was converted from posterior apical segmentectomy to larger segmentectomy (upper division segmentectomy, but not to upper lobectomy), because of his age (80 years old). Pathologic N stages were N1 in 2 patients and N2 in 1 patient. Although both patients 1 and 2 had metastasis only in the SN, patient 3 had metastasis in both SN (No. 5) and non-SN (Nos. 12 and 13). Tumors in all of the other 40 patients were classified as p-N0 by permanent sections.

There were no complications associated with radioisotope injection necessitating tube drainage, such as bleeding or severe pneumothorax. One patient had empyema 3 days after segmentectomy, which was cured by drainage and antibiotics on the 23rd postoperative day. There were no the other major complications associated with segmentectomy, including prolonged air leakage of more than 5 days. The postoperative follow-up was performed by chest and abdominal CT and brain magnetic resonance imaging every 3 months after the operation. No patients were lost to follow-up. The mean follow-up period after surgery in the 52 patients was 8 months (range: 1–15 months). Postoperative recurrence occurred in 1 patient, who underwent an apical segmentectomy of the right lower lobe for adenosquamous carcinoma 2.9 cm in size. The recurrence was at 5 months after segmentectomy, at the extraregional lymph node for tumor in the right lower lobe, that is, at the interlobar lymph node (No. 11) between the right upper lobe and middle lobe, and treated by completion pneumonectomy. During the segmentectomy of this patient, No. 13 and No. 4 were identified as SNs, which showed no metastasis in intraoperative frozen sections. The patient is now alive 11 months after the completion pneumonectomy without recurrence. The other 51 patients are also now alive without recurrence.

Discussion

The present study shows that the SN navigation segmentectomy using radioisotope tracers could increase the accuracy of intraoperative N staging and could serve as the final indication for segmentectomy. In the 3 patients with N1 or N2 disease, intraoperative frozen sections of SNs showed metastasis, which suggested the need for lobectomy. In 9 segmentectomy-treated patients whose SNs could not be identified, all hilar and lobe-specific lymph nodes were required for diagnosis, a significantly larger number than in the 43 patients whose SNs could be identified. SN identification therefore could determine a final indication for segmentectomy by targeting the lymph nodes needed for intraoperative frozen section diagnosis. In addition, serial sections of SNs during surgery might find micrometastasis more easily than single section in each of a larger number of lymph nodes.

Although the postoperative follow-up period is still short, 1 patient had local recurrence 5 months after segmentectomy. The recurrence site of this patient, however, was the extraregional lymph node. In addition, the histologic type of this patient was adenosquamous carcinoma, which is known to have poorer prognosis than other types of NSCLC.[18,19] We therefore consider that the patients with clinical T1 N0 M0 NSCLC of high malignant grade, such as adenosquamous carcinoma, large cell neuroendocrine carcinoma, adenocarcinoma with high FDG uptake on PET, and NSCLC with high carcinoembryonic antigen serum level, would be preferably treated by lobectomy rather than segmentectomy, even if the intraoperative lymph node staging is N0.

Skip metastasis to the mediastinal lymph nodes has been reported to occur in 20% to 40% of patients with NSCLC,[17,20] which could be because some lymphatic flow from the lung goes directly to the mediastinum through the pleura and not to the hilar lymph node stations.[21] The present study showed that SNs were identified in the mediastinum in 15 (35%) of 43 patients and the lymphatic route to each mediastinal lymph node station was lobe-specific.